Proc. Natl. Acad. Sci. USA
Vol. 89, pp. 9237–9241, October 1992
Biochemistry

Simian virus 40 minichromosomes as targets for retroviral integration *in vivo*

(chromatin/recombination)

PETER M. PRYCIAK*†, HANS-PETER MÜLLER‡, AND HAROLD E. VARMUS*‡

Departments of *Biochemistry and Biophysics, and ‡Microbiology and Immunology, University of California, San Francisco, CA 94143-0502

Contributed by Harold E. Varmus, May 14, 1992

ABSTRACT **We present a method for studying multiple retroviral integration events into a small DNA target *in vivo*. Episomal simian virus 40 (SV40) genomes established by infection of CV-1 cells served as integration targets during subsequent infection with murine leukemia virus (MLV). Using a PCR-based assay for the abundance and distribution of integration events, nonrandom integration of MLV DNA into SV40 DNA is detectable as early as 4 hr and reaches a maximum level by 8 hr after MLV infection. The level of integration but not the distribution of integration sites is sensitive to the stage in the SV40 life cycle at which MLV infection is performed. Using a temperature-sensitive tumor (T) antigen mutant SV40 strain, we observed that active replication of the target DNA is not required for efficient integration *in vivo*. The distribution of integration sites *in vivo* is closely approximated by *in vitro* reactions with isolated SV40 minichromosomes as integration targets. However, the degree of bias between the most and least favored sites is greater *in vivo* than *in vitro*.**

To replicate, retroviruses must insert a DNA copy of their genome into the DNA of the host cell (for reviews, see refs. 1 and 2). Integration is site-specific with regard to the retroviral DNA—invariably occurring near the termini—but is relatively nonspecific with regard to the target DNA (for reviews, see refs. 1 and 3): integration occurs at many sites and in varied target sequences both *in vivo* and *in vitro* (4–8). Nevertheless, integration sites are not chosen randomly; the distribution of sites is nonuniform, even in naked DNA *in vitro* (8–10), and can be influenced further by more complex targets, such as DNA assembled into nucleosomes (7, 8). In addition, integration *in vivo* shows a nonrandom tendency to occur near DNase I-hypersensitive sites and in transcriptionally active regions (11–14) or at certain high-frequency sites (15).

These observations have suggested that target site selection during retroviral integration *in vivo* may be sensitive to complex changes in the physiological state of DNA, such as transcription, replication, or different degrees of chromatin condensation. However, such changes are difficult to recapitulate *in vitro*, and their effects are hard to measure *in vivo* because of the large number of potential integration sites in animal cell genomes. Therefore, we have developed a system with which to study multiple integration events both *in vivo* and *in vitro* into a single, relatively small target: cells are coinfected with a DNA virus [simian virus 40 (SV40)] and a retrovirus [murine leukemia virus (MLV)], generating multiple episomal copies of SV40 DNA as integration targets for MLV (Fig. 1*A*). We find that integration of MLV DNA into SV40 minichromosomes occurs frequently *in vivo*, that target site preference is similar to that seen when using isolated SV40 minichromosomes as targets for integration *in vitro*, and that the efficiency and distribution of integration events are not appreciably dependent upon replication of the SV40 target *in vivo*.

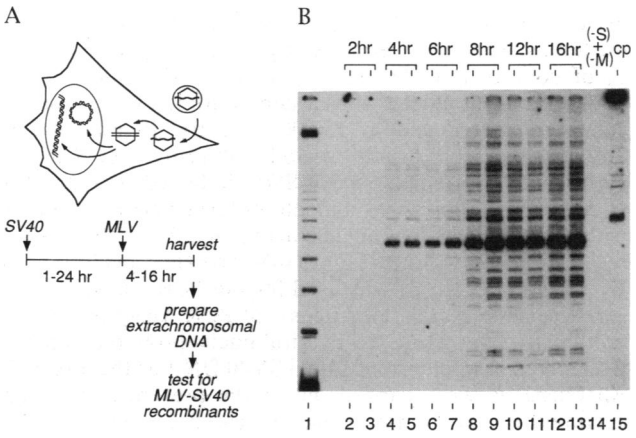

FIG. 1. MLV integration into SV40 DNA in coinfected cells. (*A*) Experimental strategy. After MLV entry into SV40-infected cells, linear double-stranded MLV DNA synthesized in nucleoprotein complexes (hexagons) can integrate into either SV40 DNA (circular double helix) or cellular chromosomal DNA (linear double helix). (*B*) Time course of integration. Duplicate plates of cells were infected with MLV 20 hr after infection with SV40, and extrachromosomal DNA was prepared at the indicated times (2 to 16 hr) after MLV infection. MLV–SV40 recombinants were amplified by polymerase chain reaction (PCR) between an end-labeled MLV long-terminal-repeat primer (MoU5L26) and an unlabeled SV40 primer (SV273+). Extrachromosomal DNAs were also harvested at the last time point from plates infected with one of the two viruses and mock-infected with the other, either MLV (-M) or SV40 (-S), and were mixed before the PCR to demonstrate that PCR products are not generated unless the cells were coinfected (lane 14). Also, PCRs were performed with a pool of 30 cloned MLV–SV40 *in vitro* recombinants, or clone pool (cp; lane 15), for which the exact positions of insertion are known (7). An end-labeled 123-base-pair (bp) ladder was also included (lane 1), with the 123-bp fragment visible at the very bottom of the gel.

MATERIALS AND METHODS

Cells and Viruses. All cells were grown in Dulbecco's modified Eagle's H-21 medium supplemented with 10% (vol/vol) fetal calf serum. The monkey cell line CV-1 served as the host for SV40 and MLV coinfections. Wild-type SV40 was strain 777; the mutant temperature-sensitive (ts) SV40 strains tsA28 and tsC219 were gifts from P. Tegtmeyer (State University of New York, Stony Brook) and M. Bina (Purdue

The publication costs of this article were defrayed in part by page charge payment. This article must therefore be hereby marked "*advertisement*" in accordance with 18 U.S.C. §1734 solely to indicate this fact.

Abbreviations: SV40, simian virus 40; MLV, murine leukemia virus; moi, multiplicity of infection; ts, temperature sensitive; PCR, polymerase chain reaction.

†Present address: Department of Genetics, SK-50, University of Washington, Seattle, WA 98195.

University), respectively. A mixture of amphotropic and ecotropic MLV was harvested from the cell line PA317:MoMLV-SupF, which was created by infecting the amphotropic packaging cell line PA317 (16) with replication competent ecotropic Moloney MLV strain MoMLV-SupF (6).

Virus Infections and Harvest of Recombinants. Duplicate plates of CV-1 cells (1×10^6 per 100-mm culture dish) were infected with wild-type SV40 [multiplicity of infection (moi) = 10, except as indicated in Fig. 2*B*] at 37°C or with SV40 ts mutants (at moi = 1; see Fig. 5 legend). Infections with MLV used fresh 24-hr harvests of virus from 5×10^6 PA317:MoMLV-SupF cells (in 4 ml) for each plate of (10^6) CV-1 cells and included 8 μg of Polybrene per ml. Coinfected cells were trypsinized and pelleted through ice-cold growth medium. Cell pellets were lysed by gentle resuspension in 150 μl of cold 10 mM Tris·HCl, pH 8.0/250 mM KCl/5 mM $MgCl_2$/0.5% Nonidet P-40. Lysates were left on ice for 2 hr and then centrifuged at 15,000 × *g* for 10 min at 4°C. Supernatants were briefly treated with proteinase K at 0.25 mg/ml in 8 mM EDTA/0.5% SDS, followed by extraction with phenol/chloroform and chloroform and precipitation with ethanol. The final nucleic acid pellet from 10^6 cells was resuspended in 40 μl of TE (10 mM Tris·HCl, pH 7.5/1 mM EDTA), and 0.5–1 μl was used for the PCR analysis (8).

***In Vitro* Integration Reactions and PCR Analysis.** Integration *in vitro* was mediated by viral nucleoprotein complexes with naked or minichromosomal SV40 DNA as the target (7). All reactions were carried out in the presence of 15 mM spermidine, except for those indicated in Fig. 3*B*. The products of reactions mediated by 20 μl of integration extract were resuspended in 20 μl of TE, and 0.5 μl was analyzed by 25 cycles of PCR (8). In all PCR reactions, the 5′-^{32}P-labeled primer was the MLV primer MoU5L26, and the target DNA primer was unlabeled. Some classes of intramolecular MLV recombinants (5) can also be detected by amplification between two MoU5L26 primers, but their low abundance in these experiments generally required 5–10 additional cycles of PCR for detection (data not shown); therefore, their presence did not affect the analysis of MLV-SV40 recombinants. The following oligonucleotides, indicated by name and map location (in parentheses), were used: MoU5L26 (8335–8360 MoMLV); SV272− (296–272 SV40); SV273+ (249–273 SV40); SV1990− (2014–1990 SV40); and SV3869− (3893–3869 SV40). The PCR products were separated in nondenaturing 5% or denaturing 6% acrylamide gels (8) and exposed to x-ray film.

RESULTS

MLV Integrates into SV40 DNA in Coinfected Cells. We infected CV-1 cells sequentially with SV40 and an amphotropic strain of MLV (Fig. 1*A*) and subsequently analyzed extrachromosomal DNA for MLV–SV40 recombinants. Initially, 12 independent recombinants were cloned (as in ref. 7), and sequencing of the MLV–SV40 junctions documented that bona fide retroviral integration had occurred at different sites in SV40 DNA (not shown). To measure both the abundance of recombinants and the distribution of insertion sites, we used a PCR-based assay (8) to amplify recombinants between an MLV primer (^{32}P-labeled at its 5′ end) and an unlabeled SV40 primer. With this method, we could observe integration products as early as 4 hr after MLV infection and maximum levels by 8 hr (Fig. 1*B*).

Pattern of MLV Integration into SV40 DNA Is Nonrandom and Not Influenced by Chronology or Multiplicity of Infection. The sizes of the PCR products indicate that MLV integrated its DNA at many positions in SV40 DNA in the region analyzed in Fig. 1*B*, but the distribution of MLV integration sites was distinctly nonrandom. Several sites were used much more frequently than others, and one site was especially favored. [The PCR assay measures true integration frequencies and not PCR amplification preferences (ref. 8; see also Fig. 3)]. Furthermore, the distribution did not change appreciably either during the accumulation of recombinants (4–8 hr) or for at least 8 hr afterwards; thus, there is no evidence for preferential replication or loss of certain recombinants during the time course of this experiment. This may occur at extended times after MLV infection (24–48 hr after MLV infection; data not shown).

We next compared the amount and distribution of integration events as a function of the stage and multiplicity of SV40 infection. When the time of MLV infection was varied from 10 hr before to 24 hr after SV40 infection (Fig. 2*A*) or the moi of SV40 was increased from 1 to 100 (Fig. 2*B*), only the number of recombinants, and not the distribution of integration sites, was affected. In both experiments, the increased number of recombinants was consistent with the increased copy number of SV40 target DNA (see Fig. 2 legend). However, no further increase in recombinants was seen when MLV infection was performed 24 rather than 12 hr after SV40 infection (Fig. 2*A*, lanes 1–4) or when the moi was raised from 10 to 100 (Fig. 2*B*, lanes 1–6), despite the greater abundance of SV40 DNA in both cases (Fig. 2 legend); this suggests either that the additional copies are not available for integration or that all of the MLV nucleoprotein complexes competent to integrate into SV40 DNA have done so at less than maximal levels of SV40 DNA.

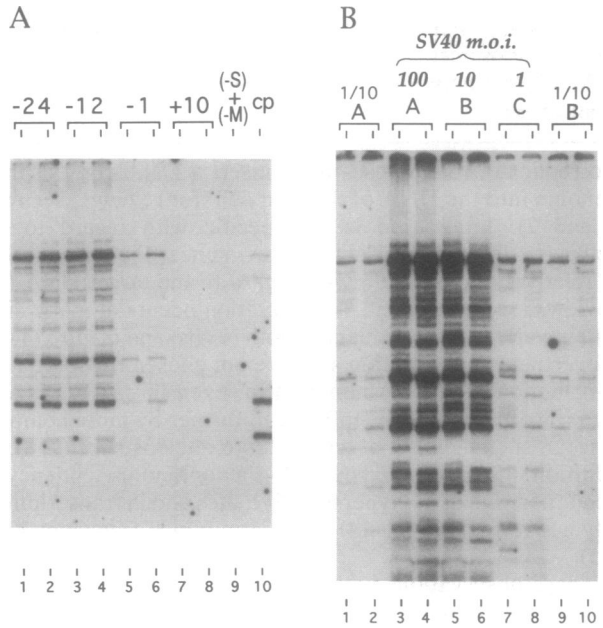

FIG. 2. Effects of the timing and multiplicity of SV40 infection upon integration of MLV DNA into SV40 DNA. (*A*) Duplicate plates of CV-1 cells were infected with SV40 (moi = 10) 24, 12, or 1 hr before (lanes 1–6) or 10 hr after (lanes 7 and 8) MLV infection, as indicated. Sixteen hours after MLV infection, extrachromosomal DNA was analyzed as in Fig. 1*B*, except that the target primer was SV1990−. The copy number of SV40 DNA at harvest was estimated by ethidium bromide staining in an agarose gel to be $\approx 10^5$, $\approx 2 \times 10^4$, $\approx 5 \times 10^2$, and $< 10^2$ per cell for the −24, −12, −1, and +10 experiments, respectively (not shown). Controls (lanes 9 and 10) were performed as in Fig. 1*B*. (*B*) Duplicate plates of CV-1 cells were infected with SV40 12 hr before MLV infection at a moi of 100, 10, or 1, for experiments A, B, and C, respectively (lanes 3–8). Recombinants were analyzed 12 hr after MLV infection as in *A*. PCRs were also performed using 1/10th the amount of some of the recombinants (set A, lanes 1 and 2; set B, lanes 9 and 10). The copy number of SV40 DNA at harvest was estimated as in *A* to be $\approx 1.5 \times 10^5$, $\approx 3 \times 10^4$, and $\approx 3 \times 10^3$ per cell for experiments A, B, and C, respectively (not shown).

Integration Target Site Selection *in Vivo* Is Closely but Not Completely Reproduced by Reactions Using Minichromosomes As Targets *in Vitro*. To ask what determines the nonuniform distribution of MLV insertions into SV40 DNA *in vivo*, we compared the products of *in vivo* integration with products of *in vitro* reactions, using naked SV40 DNA or SV40 minichromosome targets. Similar numbers of recombinants from the *in vivo* and *in vitro* integration reactions were amplified by PCR and the products were analyzed in nondenaturing gels to survey insertions over a 1- to 2-kilobase (kb) region (Fig. 3*A*) and in denaturing, high-resolution gels to survey insertions over a 300- to 400-bp region (Fig. 4).

Three general conclusions are immediately apparent from these comparisons (Figs. 3*A* and 4). First, many features of the nonrandom pattern seen *in vivo* are preserved when MLV DNA integrates into either SV40 minichromosomes or naked SV40 DNA *in vitro*. This implies that many of the site preferences that produce the *in vivo* pattern are determined simply by the sequence of SV40 DNA. Second, several features of site selection *in vivo* are more conserved during *in vitro* integration into minichromosomes than into naked DNA. These features include sites that are more highly preferred in minichromosomal DNA *in vivo* or *in vitro* than in naked DNA (e.g., solid arrowheads at positions 710, 1640, and 3705 in Figs. 3*A* and 4), sites that are used exclusively in minichromosomal DNA (e.g., filled circle at position 640), and sites that are used in naked DNA but not in minichromosomal DNA *in vitro* or *in vivo* (e.g., asterisks at positions 430, 1850, and 3550). Third, the *in vivo* and *in vitro* patterns confirm that the nucleosome-free region of SV40 DNA is not a favored site for MLV integration (7).

Although integration site selection *in vivo* can be closely reproduced *in vitro* by using minichromosomal targets, some differences remain. Most obviously, the site at position 710, which is very highly preferred *in vivo*, is less highly favored *in vitro*. In addition, a few sites that are highly preferred *in vivo* are not especially preferred *in vitro* (e.g., double arrowhead at position 1802 in Figs. 3*A* and 4). Conversely, a few sites are used preferentially *in vitro* in both naked DNA and minichromosomes but are not favored *in vivo* (e.g., open boxes at positions 320 and 3850 in Fig. 4). Thus, while a similar hierarchy of site preferences operates *in vivo* and *in vitro*, there is a greater degree of bias *in vivo* between the most and the least frequently used sites.

The higher-resolution analysis (Fig. 4) shows that most of the preferred sites (arrowheads, circle) consist of single positions, rather than regional clusters of positions. However, the sites that are poorly used in minichromosomes *in vitro* and *in vivo* (asterisks) can correspond to either single positions (lanes 4–10) or larger regions (lanes 11–17 and 18–24). Also, in contrast to our findings with other minichromosomes (8), our results with SV40 minichromosome targets do not show an obvious ≈10-bp periodic distribution of preferred sites *in vitro* or *in vivo* (see *Discussion*).

The integration site distribution *in vivo* was more closely approximated by *in vitro* reactions with minichromosome targets when performed in the presence of spermidine (Fig. 3*B*), although integration into naked SV40 DNA was relatively independent of spermidine. This dependence on spermidine differs from our observations using other minichromosomal targets (8), implying that SV40 minichromosomes may be especially prone to disassembly or rearrangement in the absence of spermidine, which can stabilize nucleosome cores (17). We also tested eight different protocols for preparing SV40 minichromosomes [by varying salt concentrations, divalent cations, lysis procedure, length of SV40 infection, and extent of purification (see ref. 18)], and all produced indistinguishable integration site distributions and equivalent dependence upon spermidine (not shown).

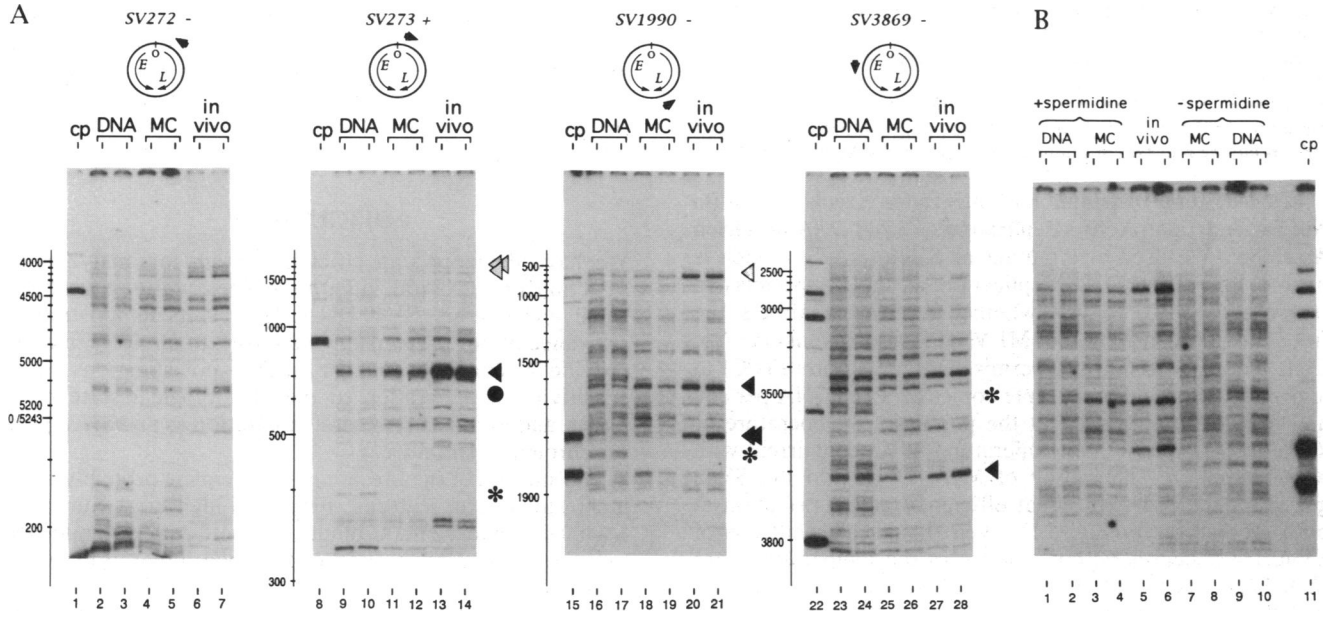

FIG. 3. Comparison of integration-site choice during *in vivo* and *in vitro* integration reactions. (*A*) PCR analysis of the products of *in vitro* integration reactions using naked SV40 DNA (DNA) or SV40 minichromosomes (lanes MC) as targets or the products of MLV integration into SV40 in coinfected cells (lanes "*in vivo*"). The clone pool (lanes cp) was used as in Fig. 1*B*. At the top are the names, positions, and orientations of the unlabeled target DNA primers (indicated as short arrows) used in the PCR reactions; in the schematic, regions of SV40 such as the origin of replication (O) and early (*E*) and late (*L*) transcription units are indicated, with map positions clockwise from the top. To the left of each panel are the map positions in SV40 DNA. Notable integration sites are indicated with symbols (single and double arrowheads, circle, asterisks; see text). Stippled single and double arrowheads indicate strong sites visible with another target primer (positions 1640 and 1802, lanes 13 and 14; and position 710, lanes 20 and 21) but are faint because of poor PCR amplification of products longer than ≈1 kb. (*B*) Duplicate *in vitro* integration reactions were performed in the presence or absence of 15 mM spermidine with either naked SV40 DNA (lanes DNA) or SV40 minichromosomes (lanes MC) as target. PCR analyses with the SV1990- target primer compared the distributions of these recombinants with those obtained by coinfection (*in vivo*). The products represented in lanes 3 and 4 were underloaded by half relative to the other *in vitro* reaction products.

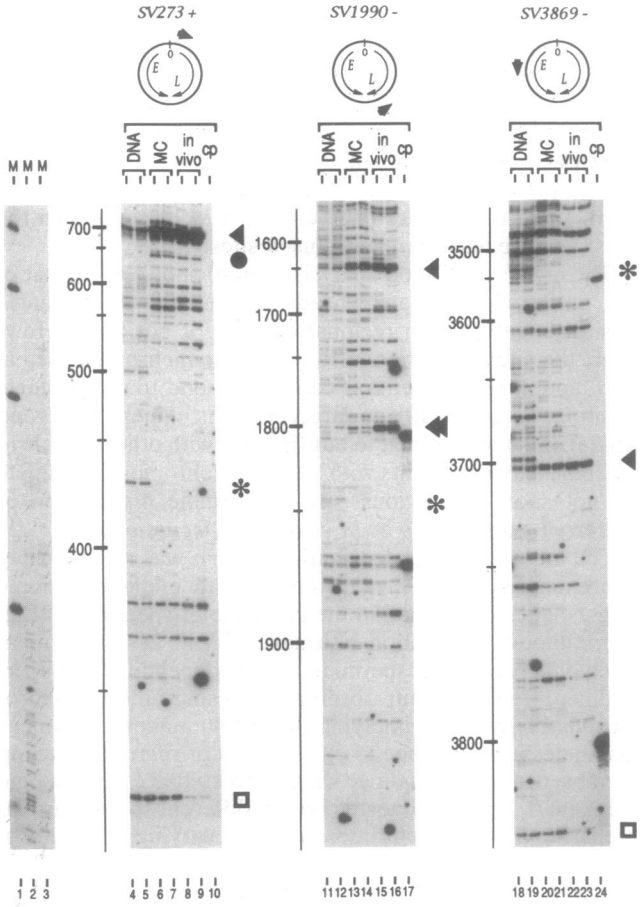

FIG. 4. Comparison of *in vivo* and *in vitro* integration-site distributions at high resolution. The same PCR products shown in Fig. 3*A* were run on a denaturing 6% polyacrylamide gel. Notable integration sites are indicated with symbols (single and double arrowheads, circle, and asterisks) as in Fig. 3*A* and as described in the text, with the addition of some (squares) that are not noted in Fig. 3*A*. Map positions in SV40 DNA are shown at the left of each panel. Size markers consisted of the clone pool (lane cp) reactions, as well as a 100-bp ladder and two sequencing ladders (lanes M, lanes 1–3).

Efficiency and Distribution of Integration Events *in Vivo* Do Not Depend Upon Active Replication of SV40 DNA or Virion Assembly. We used a ts mutant of SV40 (tsA28), which is unable to initiate DNA replication at the nonpermissive temperature (19), to ask whether replication affects the frequency or distribution of MLV integration events *in vivo*. Cells were infected at the permissive temperature (32°C) to allow accumulation of multiple copies of SV40 DNA per cell and then were either left at the permissive temperature or shifted to the restrictive temperature (40°C) concurrent with MLV infection. Integration of MLV DNA into the SV40 genome occurred with equal efficiency and distribution at both temperatures (Fig. 5*A*), even though all synthesis of SV40 DNA ceases within minutes of the temperature shift (20). This experiment also confirmed that the distribution of integration events observed does not reflect preferential replication of some of the initial integration products. Finally, there is no indication that the choice of integration sites is sensitive to the replicative status of the target. However, the fraction of total SV40 DNA that is replicating (at permissive temperature or in wild-type infections) may be small, so any replication-induced changes in integration site preference might be obscured by an excess of integration events into the nonreplicating majority of DNA.

During the late phase of the SV40 life cycle, some viral DNA is packaged into capsid structures, which may alter its accessibility to retroviral integration machinery. In experiments with a ts mutant of the major SV40 structural protein VP1 (tsC219), which cannot assemble virions at the nonpermissive temperature (21), we found that the distribution of integration sites into SV40 DNA was unaltered at the restrictive temperature (Fig. 5*B*), demonstrating that the pattern is not dependent upon virion assembly. However, since the proportion of SV40 DNA undergoing assembly at the time of MLV infection may be small, we cannot say whether or not the assembly process affects the use of SV40 DNA as an integration target.

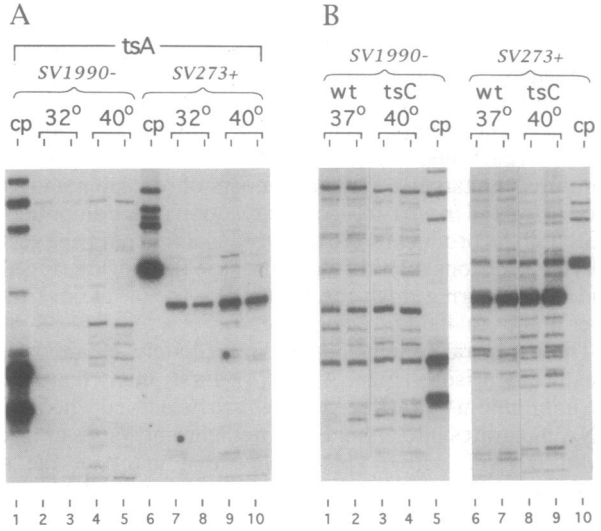

FIG. 5. Distribution of MLV integration sites does not depend on replication or packaging of SV40 DNA. (*A*) Cells were infected with the tsA28 strain of SV40 at 32°C for 24 hr and then with MLV at either 32°C or 40°C for 12 hr. Recombinants were amplified by PCR using either the SV1990− or SV273+ target DNA primer. (*B*) Cells were infected with the tsC219 strain of SV40 (lanes tsC) at 40°C for 24 hr and then with MLV at 40°C for 12 hr. To provide a standard pattern, cells were infected with wild-type SV40 (lanes wt) at 37°C for 12 hr and then with MLV for 12 hr at 37°C but not in parallel with the tsC experiment. PCR products, with either SV1990− or SV273+ primers, were analyzed for tsC and wt experiments on different gels.

DISCUSSION

We have developed an efficient system for analyzing the selection of retroviral integration sites within a relatively small *in vivo* target, SV40 DNA. The results demonstrate the relevance of our previous *in vitro* work to *in vivo* situations, provide a starting point for further investigations of the sensitivity of integration to the physiological state of the target, and establish retroviral integration as an *in vivo* probe for chromatin structure.

The success of the present experiments is probably attributable to several features. First, the high copy number of SV40 DNA may be important to compete with genomic DNA for a substantial proportion of the total integration events. Maximal integration levels were reached at 10^3 to 10^4 copies of SV40 per cell (representing ≈0.1% and ≈1% of total cell DNA, respectively; see Fig. 2). Another episome, bovine papilloma virus-based vectors present at only a few hundred copies per cell (22), can also serve as an *in vivo* integration target (H.-P.M. and H.E.V., unpublished observations). Second, it is possible that SV40 DNA competes with genomic DNA disproportionately for its fraction of total DNA mass because it is episomal, transcriptionally active, or relatively uncondensed, or perhaps because of special properties inherent to SV40 DNA. We have not yet measured the relative efficiency of integration into SV40 and chromosomal DNAs

in vivo. Conceivably, the saturation phenomenon observed in Fig. 2 could result from nearly exclusive integration into SV40 DNA. Finally, the use of extrachromosomal DNA as PCR templates lowers the nonspecific amplification that can result from the high concentration and complexity of genomic DNA (unpublished observations).

This study includes comparison (previously unreported to our knowledge) of *in vivo* and *in vitro* insertion site distributions for retroviral integration into a single target. We previously observed that integration does not occur preferentially in nucleosome-free and/or nuclease-sensitive regions in minichromosome targets *in vitro* (7, 8). Here we observe that the integration machinery also does not display such a preference *in vivo*. Instead, many sites are available for integration throughout the SV40 genome *in vivo*, and the most frequently used sites were within the transcribed, coding regions assembled into nucleosomes (Fig. 3*A*).

The *in vivo* integration-site distributions did exhibit some differences from those of the *in vitro* reactions. Bias between strong and weak sites *in vitro* is further accentuated *in vivo*, suggesting either that the target is simply more homogeneous or ordered *in vivo* or that it is in a qualitatively different state or environment *in vivo* than *in vitro*. We showed previously that assembly of DNA into nucleosomes can cause increased bias between sites by both inhibition and enhancement of site reactivities and can promote an ≈10-bp periodic distribution of preferred sites (8). For SV40 targets, the differences between naked and nucleosomal DNA are less striking than with the previously used targets, and no periodicity was observed (Fig. 4). The nucleosomes in SV40 minichromosomes apparently do not exhibit the strict rotational positioning necessary to observe periodic usage. The large number of nucleosomes on SV40 DNA (20–27 total) are poorly phased translationally (ref. 23, and references therein), perhaps limiting the ability of individual nucleosomes to assume preferred rotational orientations (24, 25).

These experiments provide a starting point for further manipulations of the physiological state of target DNA *in vivo* and study of the resulting effects on integration. Thus, by using a tsA strain of SV40, we were able to demonstrate that, as during *in vitro* reactions, active replication is not required for DNA to serve as a good integration target *in vivo*. This observation helps to distinguish among explanations for several earlier experiments in which integration occurred principally into recently replicated DNA or was inhibited in cells in which cellular DNA synthesis was blocked (26–28). The lack of a direct requirement for active replication of an integration target *in vivo* is consistent with recent experiments demonstrating that integration of MLV DNA requires passage of the infected cell through mitosis (T. Roe, T. Reynolds, and P. Brown, personal communication), explaining earlier observations. A cell cycle requirement for integration may imply that, in our experiments, MLV integration into SV40 DNA will only occur in the fraction of cells that are infected with MLV before SV40 halts the cell cycle (29–31).

We thank M. Bina and P. Tegtmeyer for ts SV40 stocks and J. Cox and B. Liu for help with early stages of this work. We also thank T. Roe, T. Reynolds, and P. Brown for permission to cite their unpublished work, and M. Botchan and P. Brown for critical readings of the manuscript. This work was supported by a grant from the National Institutes of Health to H.E.V. and by a fellowship from the Swiss National Science Foundation to H.-P.M. H.E.V. is an American Cancer Society Research Professor.

1. Varmus, H. E. & Brown, P. (1989) in *Mobile DNA*, eds. Berg, D. E. & Howe, M. M. (Am. Soc. Microbiol., Washington), pp. 53–108.
2. Whitcomb, J. M. & Hughes, S. H. (1992) *Annu. Rev. Cell Biol.*, in press.
3. Sandmeyer, S. B., Hansen, L. J. & Chalker, D. L. (1990) *Annu. Rev. Genet.* **24**, 491–518.
4. Shimotohno, K. & Temin, H. M. (1980) *Proc. Natl. Acad. Sci. USA* **77**, 7357–7361.
5. Shoemaker, C., Hoffmann, J., Goff, S. P. & Baltimore, D. (1981) *J. Virol.* **40**, 164–172.
6. Brown, P. O., Bowerman, B., Varmus, H. E. & Bishop, J. M. (1987) *Cell* **49**, 347–356.
7. Pryciak, P. M., Sil, A. & Varmus, H. E. (1992) *EMBO J.* **11**, 291–303.
8. Pryciak, P. M. & Varmus, H. E. (1992) *Cell* **69**, 769–780.
9. Leavitt, A. D., Rose, R. B. & Varmus, H. E. (1992) *J. Virol.* **66**, 2359–2368.
10. Kitamura, Y., Lee, Y. M. A. & Coffin, J. M. (1992) *Proc. Natl. Acad. Sci. USA* **89**, 5532–5536.
11. Vijaya, S., Steffen, D. L. & Robinson, H. L. (1986) *J. Virol.* **60**, 683–692.
12. Rohdewohld, H., Weiher, H., Reik, W., Jaenisch, R. & Breindl, M. (1987) *J. Virol.* **61**, 336–343.
13. Scherdin, U., Rhodes, K. & Breindl, M. (1990) *J. Virol.* **64**, 907–912.
14. Mooslehner, K., Karls, U. & Harbers, K. (1990) *J. Virol.* **64**, 3056–3058.
15. Shih, C.-C., Stoye, J. P. & Coffin, J. M. (1988) *Cell* **53**, 531–537.
16. Miller, A. D. & Buttimore, C. (1986) *Mol. Cell. Biol.* **6**, 2895–2902.
17. Morgan, J. E., Blankenship, J. W. & Matthews, H. R. (1987) *Biochemistry* **26**, 3643–3649.
18. Oudet, P., Weiss, E. & Regnier, E. (1989) *Methods Enzymol.* **170**, 14–25.
19. Loeber, G., Tevethia, M. J., Schwedes, J. F. & Tegtmeyer, P. (1989) *J. Virol.* **63**, 4426–4430.
20. Chou, J. Y., Avila, J. & Martin, R. G. (1974) *J. Virol.* **14**, 116–124.
21. Bina, M., Blasquez, V., Ng, S.-C. & Beecher, S. (1983) *Cold Spring Harbor Symp. Quant. Biol.* **47**, 565–569.
22. Richard-Foy, H. & Hager, G. L. (1987) *EMBO J.* **6**, 2321–2328.
23. Ambrose, C., Lowman, H., Rajadhyaksha, A., Blasquez, V. & Bina, M. (1990) *J. Mol. Biol.* **214**, 875–884.
24. Drew, H. R. & McCall, M. J. (1987) *J. Mol. Biol.* **197**, 485–511.
25. Drew, H. R. & Calladine, C. R. (1987) *J. Mol. Biol.* **195**, 143–173.
26. Varmus, H. E., Padgett, T., Heasley, S., Simon, G. & Bishop, J. M. (1977) *Cell* **11**, 307–319.
27. Hsu, T. W. & Taylor, J. M. (1982) *J. Virol.* **44**, 493–498.
28. Chinsky, J. & Soeiro, R. (1982) *J. Virol.* **43**, 182–190.
29. Pages, J., Manteuil, S., Stehelin, D., Fiszman, M., Marx, M. & Girard, M. (1973) *J. Virol.* **12**, 99–107.
30. Gershey, E. L. (1979) *J. Virol.* **30**, 76–83.
31. Hiscott, J. B. & Defendi, V. (1979) *J. Virol.* **30**, 590–599.